Materials Science and Engineering, A186 (1994) 157–162

Reversibility of the allotriomorphic ferrite and austenite transformations

S. Suzuki and H. K. D. H. Bhadeshia

University of Cambridge/JRDC, Department of Materials Science and Metallurgy, Pembroke Street, Cambridge CB2 3QZ (UK)

(Received August 18, 1993; in revised form November 17, 1993)

Abstract

The reversibility of the austenite (γ) to allotriomorphic ferrite (α) transformation has been investigated with a view to assessing the hysteresis. It is confirmed that the transformation can be easily reversed, a reflection of the fact that the mechanism of transformation ensures that the transformation products when they first form are close to equilibrium. The hysteresis has been shown to be much smaller than is found to be the case with the bainite reaction. Furthermore, the formation of austenite occurs with a much smaller hysteresis than that of ferrite, because the former transformation tends to occur at higher temperatures.

1. Introduction

The reversibility of a phase transformation can reveal interesting information about the state of equilibrium at the transformation interface and about the detailed mechanism of transformation. For example, the growth of bainite is considered to occur without diffusion, with the excess carbon being partitioned into the residual austenite soon after growth. This makes the transformation irreversible so that a large amount of superheating is required before austenite reforms [1–3]. By contrast, carbon partitions *during* the growth of allotriomorphic ferrite so that any hysteresis during reversion should be smaller [4, 5].

The purpose of this work was to study the formation of allotriomorphic ferrite from a mixed microstructure of allotriomorphic ferrite and austenite. In this way, the nucleation of ferrite is rendered unnecessary. It was intended to verify that the hysteresis associated with the transformation is much smaller than that associated with bainite. The alloy studied is an Fe–C–Si–Mn–Nb steel of technological importance in the context of accelerated cooled steels.

2. Experimental procedure

A Fe–0.16C–0.45Si–1.45Mn–0.040Nb wt.% alloy was used to study the reversibility of allotriomorphic ferrite and austenite transformation. The calculated time–temperature–transformation (TTT) diagram [6, 7] of the alloy is shown in Fig. 1. Phase fractions for the equilibrium state, calculated using Thermo-Calc [8], are also shown in Fig. 2. In Fig. 2 the fraction of NbC is not shown because it is quite small (for example, 4.8×10^{-4} at 800 °C). The alloy was provided by SOLLAC in a normalized state, and machined into cylindrical specimens, each of diameter 8 mm and length 12 mm. All dilatometry was conducted on a Thermecmaster-Z thermomechanical simulator, which monitors and records time, temperature and radial strain during heat treatment. Specimens were heated using radio-frequency induction, and He gas was used to control the cooling rate. A schematic illustration of the arrangement is shown in Fig. 3.

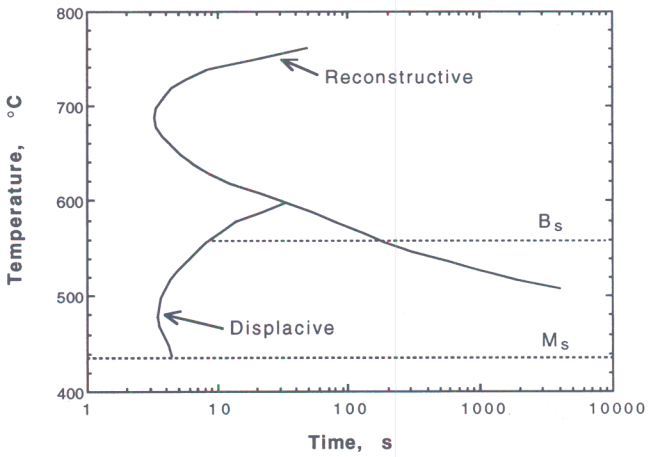

Fig. 1. Calculated time–temperature–transformation (TTT) diagram of the alloy used.

0921-5093/94/$7.00
SSDI 0921-5093(93)09485-2

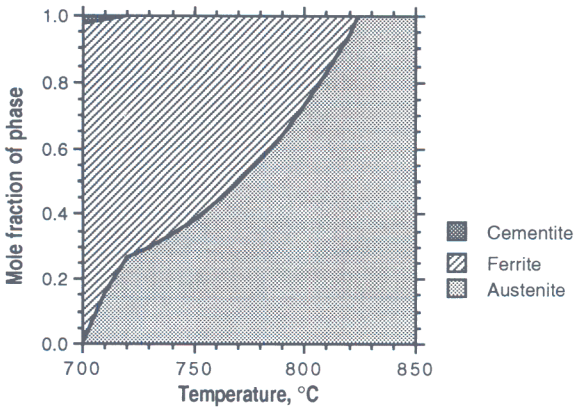

Fig. 2. Equilibrium phase fractions calculated using Thermo-Calc.

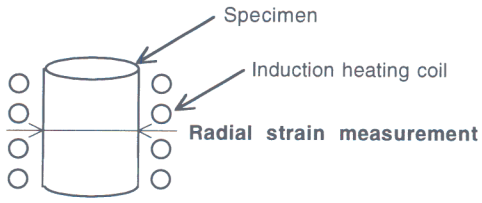

Fig. 3. Schematic illustration of experiment with Thermecmaster-Z.

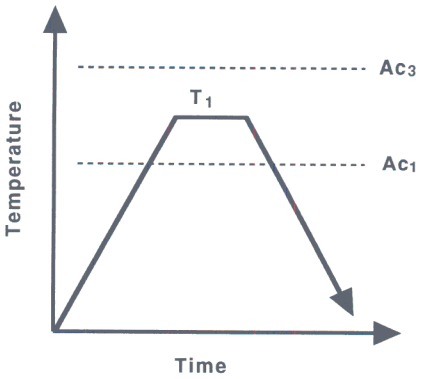

Fig. 4. Schematic illustration of the heat treatment.

TABLE 1. Measured and calculated transformation temperatures

Heating/cooling rate (°C s^{-1})	Ac_1 (°C)	Ar_1 (°C)	Ac_3 (°C)	Ar_3 (°C)
1.0	712	530	850	750
0.1	705	585	830	775
Equilibrium	700 °C (Ae_1)		825 °C (Ae_3)	

To study the reversibility of the allotriomorphic ferrite reaction, beginning with a mixture of allotriomorphic ferrite and austenite, specimens were first heated up to 900 °C for 120 s, in the single-phase austenite region, and then cooled down to room temperature to detect the Ac_1, Ac_3, Ar_1, Ar_3 temperatures. These temperatures represent the austenite transformation start and finish temperatures, and the ferrite transformation start and finish temperatures respectively. Two different heating/cooling rates of 1.0 °C s^{-1} and 0.1 °C s^{-1} were utilized. This particular procedure ensures a consistent starting microstructure. The heating was stopped at temperatures of T_1, and a variety of T_1 values were studied with $T_1 = 830$, 810 or 800 °C. All of these are between the Ac_1 and Ac_3 temperatures, in order to ensure a mixed structure of allotriomorphic ferrite and austenite when cooled continuously at the rate of 1.0 °C s^{-1}. For the heating/cooling rate of 0.1 °C s^{-1}, corresponding values of $T_1 = 790$ or 760 °C were chosen because a smaller superheat is then needed for transformation to occur. At each maximum temperature of T_1, the specimen was held for 30 s in order to allow the phase fractions to stabilize. The heat treatment cycles are shown in Fig. 4.

3. Results

Table 1 shows the measured transformation temperatures. The temperature below which austenite does not exist at equilibrium (Ae_1) and that above which the steel becomes fully austenitic (Ae_3) were calculated using Thermo-Calc. As expected, $Ac_1 > Ae_1$, $Ac_3 > Ae_3$ and $Ar_1 < Ae_1$, $Ar_3 < Ae_3$, the inequalities becoming smaller as the rate of temperature change was reduced.

Figure 5 shows the radial strain observed during the heat treatment at 1.0 °C s^{-1} for various values of T_1 (maximum heating temperature). As T_1 was reduced, the allotriomorphic ferrite transformation began at higher temperature (that is, Ar_3 became higher), and the "valley" of strain around Ar_3 was found to become smaller. Figure 6 shows the observed radial strains during the heat treatment at 0.1 °C s^{-1}. In this case, allotriomorphic ferrite formation occurs soon after the cooling starts, and there is no valley of strain around Ar_3.

From Fig. 5, the volume fraction of austenite during the heat cycle was calculated presuming the line for the thermal expansion of austenite from the experiment in which T_1 was set at 900 °C as shown in Fig. 7 [9]. Figure 8 shows the relationship between temperature and the measured volume fraction of austenite during heating and cooling for $T_1 = 900$ °C for heating and cooling rates of 1.0 °C s^{-1}. The calculated austenite fraction for equilibrium is also shown in Fig. 8. During heating the volume fraction of austenite is found to be smaller than that expected for equilibrium at any temperature, and it is larger than for equilibrium during cooling. It is noticeable that the amount of austenite during heating is closer to equilibrium than that for

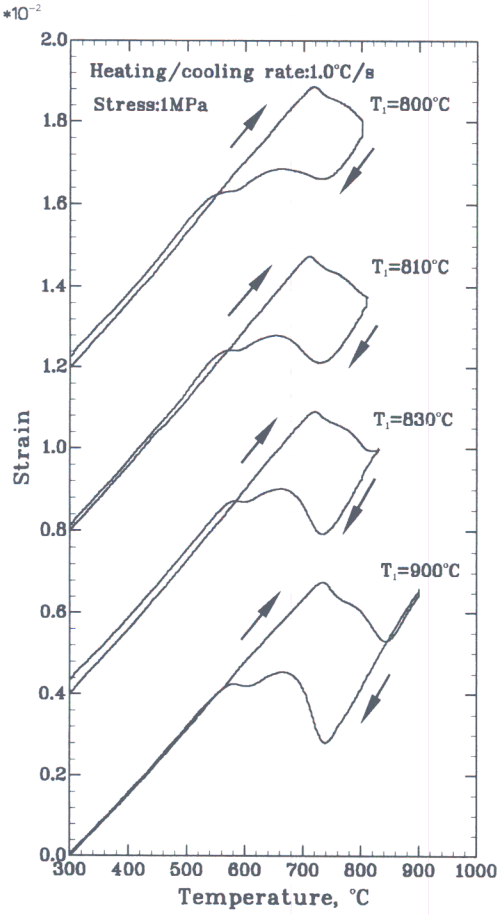

Fig. 5. Strains for $|dT/dt| = 1.0\,°C\,s^{-1}$ and a variety of values of T_1.

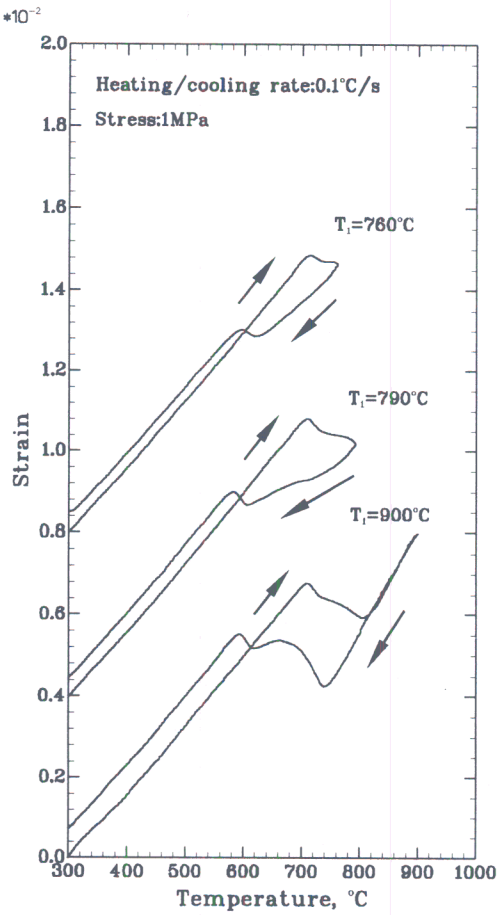

Fig. 6. Strains for $|dT/dt| = 0.1\,°C\,s^{-1}$ and a variety of values of T_1.

cooling. This is probably because the formation of austenite during heating occurs at higher temperatures where atomic mobility is larger; the transformation temperature ranges during heating and cooling are, respectively, 720–850 °C and 530–750 °C. Also, because of the low alloy concentration in the steel studied, the difference between the equilibrium and the para-equilibrium phase fractions is not expected to be large.

Figure 9 shows the volume fraction of austenite as a function of cooling for a variety of values of T_1. As T_1 decreases, the austenite volume fraction at T_1 also decreases and the austenite fraction begins to change at higher temperatures during the cooling part of the cycle. It is very interesting that the volume fraction of austenite at T_1 has a value that is close to equilibrium, even though it lags behind equilibrium during heating. This is because the $\alpha \rightarrow \gamma$ transformation proceeds substantially towards equilibrium while holding at T_1 for just 30 s. This rather rapid approach towards the equilibrium volume fraction of austenite does not necessarily imply that the equilibrium phase compositions are achieved.

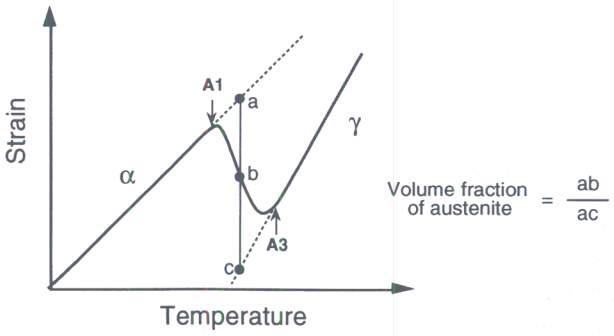

Fig. 7. Method of calculating the volume fraction of austenite [9].

The relationship between T_1 and Ar_3 is shown in Fig. 10. As T_1 decreases, Ar_3 increases gradually. The hysteresis, defined as $T_1 - Ar_3$ between T_1 and Ar_3 is also shown in Fig. 10. The Ac_3 temperature of the alloy for heating at a rate of 1.0 °C s^{-1} is 850 °C, so once the alloy becomes fully austenitic ($T_1 > 850$ °C), the Ar_3 temperature will only be a function of the austenite grain size.

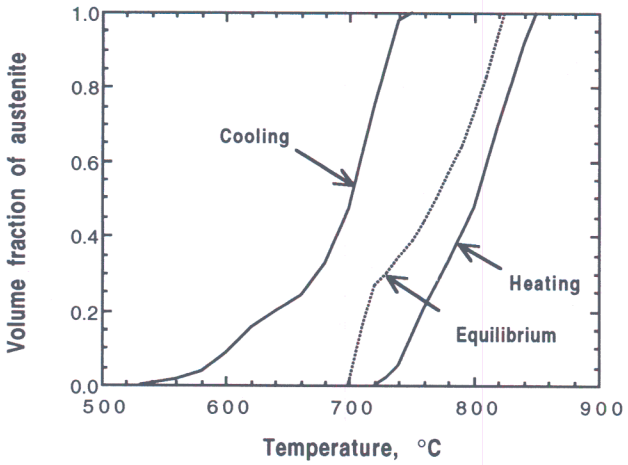

Fig. 8. Volume fraction of austenite for heating, cooling and equilibrium for heating/cooling rate of 1.0 °C s^{-1}.

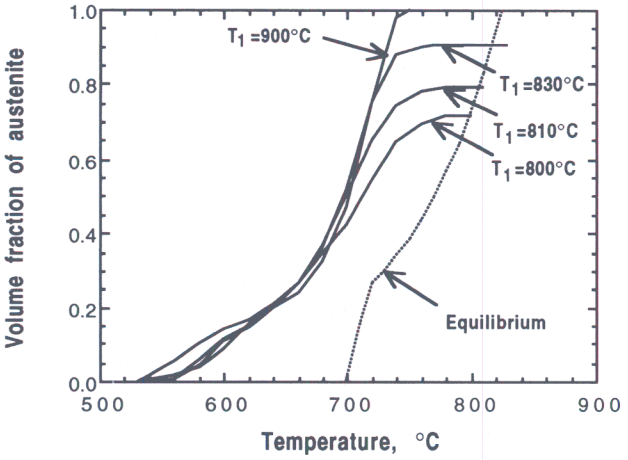

Fig. 9. Volume fraction of austenite during cooling for various values of T_1 for heating/cooling rate of 1.0 °C s^{-1}.

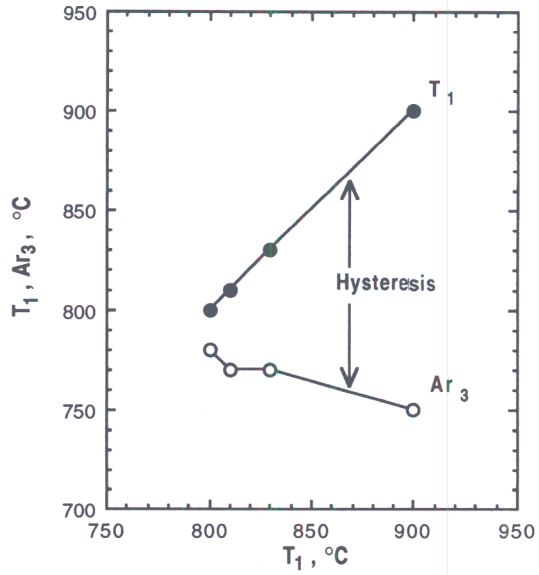

Fig. 10. Relationship between T_1, Ar_3 and hysteresis for heating/cooling rate of 1.0 °C s^{-1}. The alloy is fully austenitic for $T_1 \geq 850$ °C.

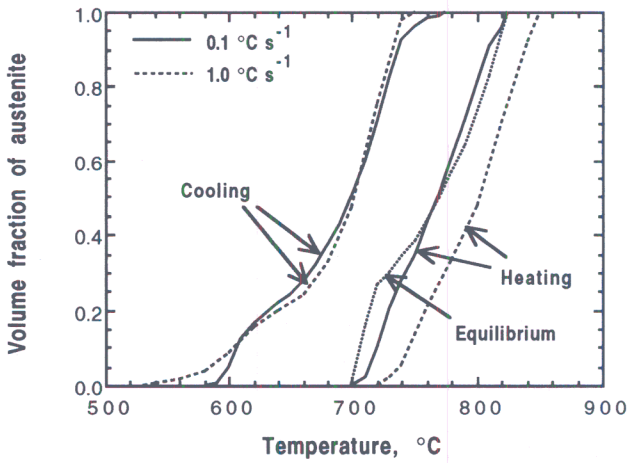

Fig. 11. Volume fraction of austenite for heating, cooling and equilibrium for heating/cooling rates of 1.0 and 0.1 °C s^{-1}.

Figure 11 shows the volume fraction of austenite for the heating/cooling rate of 0.1 °C s^{-1} measured as shown in Fig. 7 and the calculated equilibrium austenite volume fraction, compared with that for a heating/cooling rate of 1.0 °C s^{-1}. The austenite fraction during heating is found to be very close to that expected from equilibrium. This is consistent with the much slower heating rate. Surprisingly, the austenite fraction during cooling shows no significant change compared with the experiments in which the cooling rate is 1.0 °C s^{-1} except below 600 °C. Figure 12 shows the changes in austenite volume fraction change as a function of T_1. When the temperature begins to decrease, the allotriomorphic ferrite transformation starts without any delay for $T_1 = 790$ and 760 °C, where ferrite nucleation is not necessary (that is, there is no hysteresis). As the temperature goes down, the volume fraction of austenite becomes close to that of $T_1 = 900$ °C because the slope of austenite volume fraction becomes gentle as T_1 decreases. The relationship between T_1, Ar_3 and hysteresis is shown in Fig. 13. The points for $T_1 = 830$ °C ($= Ar_3$) are plotted in the figure for the same reason as before. In this case T_1 has the same value with Ar_3 below 790 °C, which means that there is zero hysteresis for the $\alpha + \gamma \rightarrow \alpha$ transformation.

4. Discussion

In the majority of experiments reported here, the starting microstructure always contained allotriomorphic ferrite, so that its nucleation was not necessary. This is useful as it makes interpretation easier.

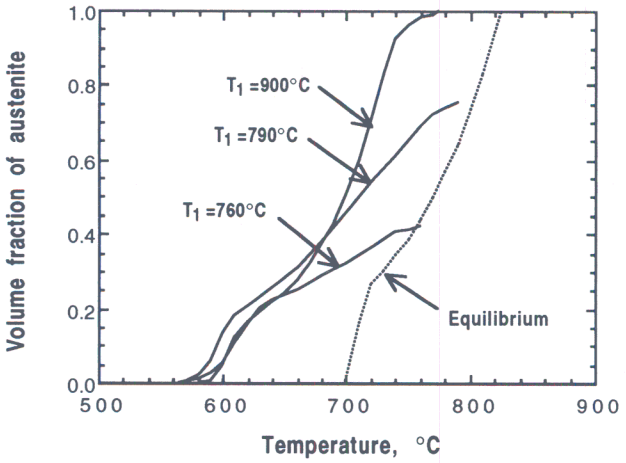

Fig. 12. Volume fraction of austenite during cooling for various values of T_1 for heating/cooling rate of 0.1 °C s^{-1}.

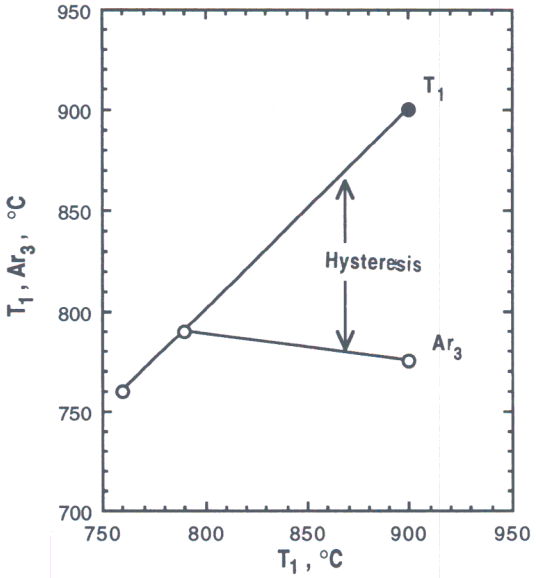

Fig. 13. Relationship between T_1, Ar_3 and hysteresis for heating/cooling rate of 0.1 °C s^{-1}.

The experiments show that the hysteresis between the reheating temperature (T_1) and the allotriomorphic ferrite transformation start temperature (Ar_3) becomes smaller as T_1 decreases; that is, where there is a mixed starting microstructure of allotriomorphic ferrite and austenite. Moreover, by reducing the cooling rate the hysteresis can be eliminated altogether. This is because there is no need for allotriomorphic ferrite to nucleate, and also because the cooling rate is small enough to allow reconstructive transformation as the temperature decreases. This small hysteresis needed for the reversal of transformation is a reflection of the fact that allotriomorphic ferrite is close to equilibrium when it first forms.

This is in contrast to the diffusionless growth of bainite, in which the subsequent partitioning of carbon renders the transformation irreversible in the thermodynamic sense. The maximum fraction of bainite is restricted by the T_0 curve so that the residual austenite cannot achieve its equilibrium carbon concentration. It then has to be superheated substantially (until the composition of the austenite reaches the Ae_3 boundary) before reverse transformation becomes thermodynamically possible.

It is also notable from Figs. 9 and 12 that, as T_1 decreases, the rate at which ferrite forms during cooling also decreases. This means that the growth of allotriomorphic ferrite is slower with lower T_1, even though there are more nuclei. As T_1 is reduced, the concentration of carbon in the residual austenite increases in a way consistent with the Ae_3 phase boundary. Consequently, the carbon concentration gradients that develop during the subsequent growth of ferrite must be smaller, and hence the growth rate of ferrite is expected to be retarded.

5. Conclusions

Transformation experiments have been conducted in which the nucleation of phases is not required. It has been demonstrated that, in these circumstances, the hysteresis associated with the formation of allotriomorphic ferrite can be rather small or zero. This is because the ferrite is quite close to equilibrium when it first forms compared with bainite, for which the hysteresis has been reported to be much larger.

When austenite grows by reconstructive transformation, the hysteresis is demonstrated to be much smaller than that associated with the growth of allotriomorphic ferrite. This is because the austenite growth tends to occur at higher temperatures.

Acknowledgments

The authors are grateful to Professor C. J. Humphreys for the provision of laboratory facilities at the University of Cambridge. S.S. gratefully acknowledges the support of the NKK Corporation (Japan). H.K.D.H.B.'s contribution to this work was made under the auspices of the Atomic Arrangements: Design and Control Project, which is a collaborative effort between the University of Cambridge and the Research and Development Corporation of Japan.

References

1 J. R. Yang and H. K. D. H. Bhadeshia, in J. Y. Koo (ed.), *Proc. Int. Conf. on Welding Metallurgy of Structural Steel, Denver, CO, 1987.* TMS, Warrendale, PA, 1987, pp. 549–563.

2 J. R. Yang and H. K. D. H. Bhadeshia, in G. W. Lorimer (ed.), *Proc. Int. Conf. Phase Transformations '87, Cambridge, UK, 1987*, Institute of Metals, London, 1988, pp. 203–206.
3 J. R. Yang and H. K. D. H. Bhadeshia, *Mater. Sci. Eng., A131* (1991) 99.
4 H. K. D. H. Bhadeshia, *Bainite in Steels*, The Institute of Materials, London, 1992.
5 K. Tsuzaki, K. Yamaguchi, T. Maki and I. Tamura, *Tetsu-to-Hagane, 74* (1988) 1430.
6 H. K. D. H. Bhadeshia, *Acta Metall., 29* (1981) 1117.
7 H. K. D. H. Bhadeshia, *Met. Sci., 16* (1982) 159.
8 Thermo-Calc, Royal Institute of Technology, Sweden, 1985.
9 M. Takahashi and H. K. D. H. Bhadeshia, *J. Mater. Sci. Lett., 8* (1989) 477.